Significant Enhancement of Triboelectric Charge Density by Fluorinated Surface Modification in Nanoscale for Converting Mechanical Energy

Hua Yang Li, Li Su, Shuang Yang Kuang, Cao Feng Pan, Guang Zhu, and Zhong Lin Wang*

Excellent triboelectric and mechanical properties are achieved on the same material for the first time by developing an effective, general, straightforward, and area-scalable approach to surface modification of a polyethylene terephthalate (PET) film via inductive-coupled plasma etching. The modification enables gigantic enhancement of triboelectric charge density on the PET surface. Based on the modified PET as a contact material, a triboelectric nanogenerator (TENG) exhibits significantly promoted electric output compared to the one without the modification. The obtained electric output is even superior to a TENG made of conventional polytetrafluoroethylene that is known for its strongest ability of being charged by triboelectrification among all engineering plastics. Detailed characterizations reveal that the enhancement of triboelectric charge density on the PET is attributed to both chemical modification of fluorination and physical modification of roughened morphology in nanoscale. Therefore, this work proposes a new route to obtaining high-performance TENGs by manipulating and modifying surface properties of materials.

1. Introduction

Contact electrification is a common phenomenon in which charge transfer takes place between two dissimilar materials at the contact interface. It has been recently utilized in triboelectric nanogenerators (TENGs) to harvest ambient mechanical energy.[1] This technology received extensive attentions due to its prominent advantages such as high power density and the ability of harnessing various kinds of mechanical motions.[2–7] An important factor that linearly relates to the output power of a TENG is the density of triboelectric charge at the contact interface between the two materials.[8,9] As a result, to obtain high-level electric output, a pair of materials that have large difference in the triboelectric series was purposely selected,[1,10] one at the positive end while the other at the negative end. For materials having strong abilities of gaining negative triboelectric charge, they normally carry halogen elements especially fluorine that has a high electron affinity.[11,12] Typical examples include polyvinyl chloride (PVC), fluorinated ethylene propylene, and polytetrafluoroethylene (PTFE). Most previously reported TENGs utilized these commercially available engineering polymeric materials,[2,6] whereas material modification in purpose was rarely reported. The use of conventional polymeric materials has apparent limitations. On one hand, fluorinated materials such as PTFE need harsh conditions for synthesis and molding.[13] Furthermore, their mechanical properties are poor in terms of elastic modulus.[14] On the other hand, polymeric materials of good mechanical properties, such as polyethylene terephthalate (PET), do not excel in being charged by triboelectrification.[1,12] Therefore, it is greatly desirable to realize the two aforementioned merits on a single material that not only owns excellent mechanical strength but also can be easily charged.

Here we report effective surface modification on PET film, which realizes significant enhancement of triboelectric charge density for high-performance TENGs. The modification is carried out by inductive-coupled plasma etching using mixture of carbon tetrafluoride (CF_4) and oxygen (O_2) gases. TENGs based on the modified PET exhibit a drastic enhancement of some 300% in open-circuit voltage, short-circuit current, and induced charge quantity. The electric output even surpasses TENGs based on conventional PTFE film of the same thickness. Detailed characterization results indicate that the promotion of triboelectric charge density is attributed to both chemical modification by fluorination and physical modification by roughened surface morphology in nanoscale. Furthermore, the surface treatment method for the modification is straightforward and scalable. Therefore, this work proposes a new route to obtaining high-performance TENGs by manipulating properties of materials.

H. Y. Li, Dr. L. Su, S. Y. Kuang, Prof. C. F. Pan, Prof. G. Zhu, Prof. Z. L. Wang
Beijing Institute of Nanoenergy and Nanosystems
Chinese Academy of Sciences
Beijing 100083, P.R. China
E-mail: zhuguang@binn.cas.cn
Prof. Z. L. Wang
School of Materials Science and Engineering
Georgia Institute of Technology
Atlanta, GA 30332, USA

DOI: 10.1002/adfm.201502318

2. Results and Discussions

2.1. Surface Modification by Plasma Etching

PET is a frequently used engineering plastic due to its good mechanical strength, hardness, and chemical resistance. The rigidity and strength are attributed to the benzene ring in the molecular main chain. Besides, it can be synthesized, processed, and molded in relatively mild conditions compared to those fluorinated polymers. A bare and precleaned PET film of 50 μm in thickness was treated under inductive-coupled plasma (ICP, SENTECH SI500) for 2 min (**Figure 1**a), making the surface modified, as shown in Figure 1b. Water contact angle measurement shows the transition from hydrophilic surface (74° in Figure 1c) to hydrophobic surface (114° in Figure 1d) upon the modification. The change is attributed to the addition of hydrophobic fluorine-contained groups onto the PET surface, which will be discussed below. The treated PET film still exhibits flexibility and transparency like a bare PET film (inset in Figure 1e). Alteration of optical transmission was not observed in the visible light region, which is shown in Figure 1e. To fabricate a complete TENG, copper electrode was then deposited onto the back surface of the modified PET by sputtering. Subsequently, another copper electrode was used to construct a TENG that has contact mode.[7,15] Each side was fixed on a substrate, as depicted in Figure 1f. The size of the device is 25 mm × 25 mm. Repeated contacts between the two sides generate alternating flows of induced electrons between the two electrodes (Figure 1f).[1,7] The metal electrode acts as a donor of negative charge when in contact with the modified PET. How much negative charge gained by the PET per unit apparent area determines the electric output of a TENG. The detailed treatment parameters are presented in Experimental Section.

2.2. Enhanced Electric Output of TENG

To investigate the influence of the modification on a TENG's electric output, we fabricated three types of devices for comparison. In addition to the TENG based on the modified PET, the other two groups are made from bare PET and PTFE films of the same thickness, respectively. The results of electric measurement are presented in **Figure 2**, which include open-circuit voltage (V_{oc}), short-circuit current (I_{sc}), and total induced charge carried by a current peak.[6,7] It can be obviously obtained that the TENG using the modified PET produces significantly enhanced electric output compared to the one without modification. The V_{oc}, I_{sc}, and induced charge all increase by approximately twofolds, which are respectively shown in Figure 2a–c. It was surprisingly found that the electric output after modification is even superior to that from PTFE-based TENGs, even though PTFE is considered as the material that has the strongest ability of gaining negative triboelectric charge.[1] An enhancement by over 50% can be obtained from the data in Figure 2. This seemingly counter-intuitive result is caused by the physical modification of surface morphology in nanoscale, which will be discussed below. Therefore, the modification enables a new route to obtaining high-level TENGs by materials engineering instead of just materials selection. The origin of the highly improved electric output lies in the enhanced triboelectric charge density on the modified PET surface. We used Kelvin probe force microscope (KPFM, Park System NX-10) to investigate the electric potential of a surface that is rubbed by an atomic force microscope (AFM) tip in microscale. As shown in **Figure 3**a,b, the average surface potential of the unmodified and modified films is 41 and 105 mV, respectively. The distinction of the surface potential originates from largely altered triboelectric charge density, i.e., surface charge per unit apparent surface area. Based on the fundamental mechanism of contact

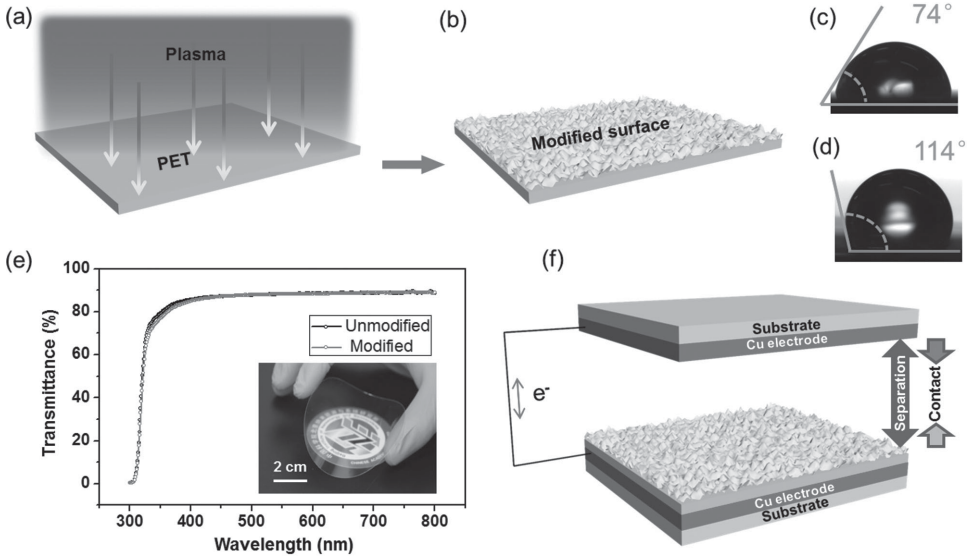

Figure 1. Surface modification on a PET film and its use in TENG. a) Illustration of the modification by inductive-coupled plasma etching; b) schematic of a modified surface; c) water contact angle on a bare PET surface; d) water contact angle on a modified PET surface; e) optical transmission of an unmodified and a modified PET sample (inset: photograph of a modified sample); and f) structure of a triboelectric nanogenerator that uses the modified PET as a contact material.

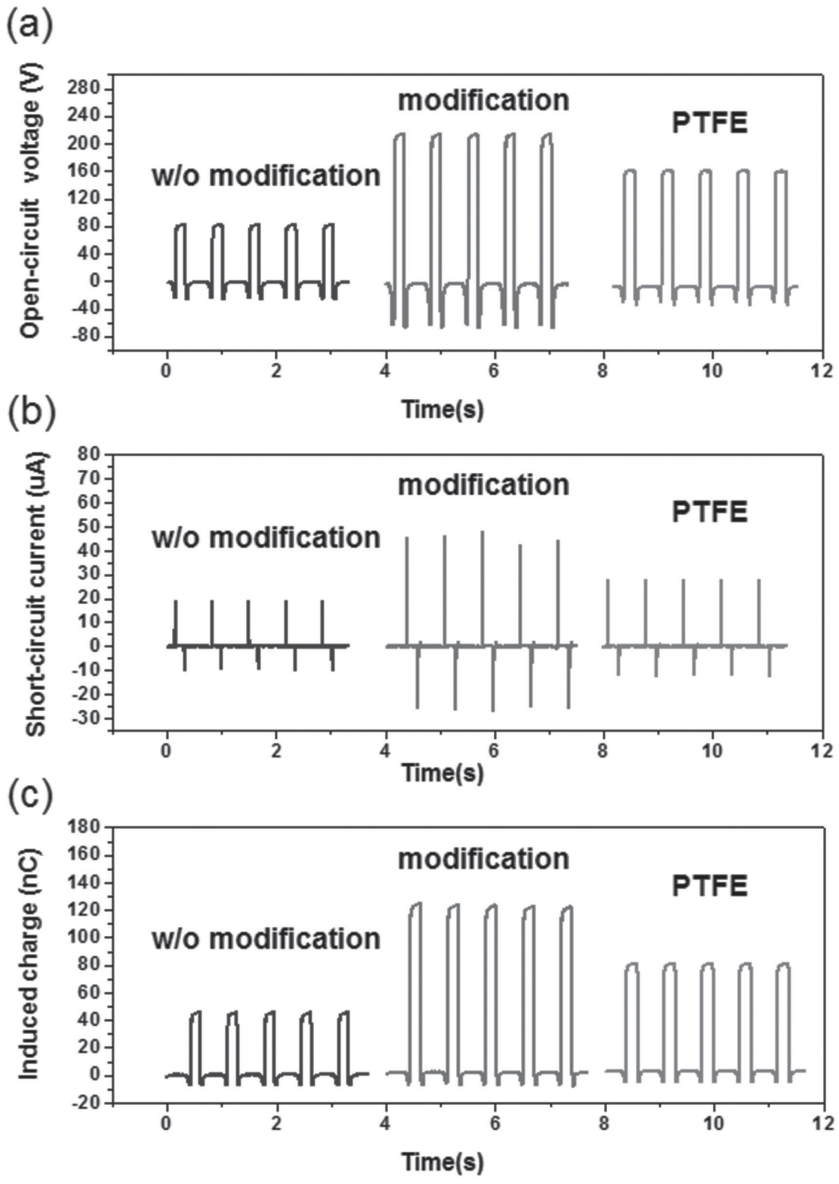

Figure 2. Electric measurement results that exhibit significant enhancement. a) Open-circuit voltage, b) short-circuit current, and c) induced charge quantity of three TENGs that used bare PET, modified PET and PTFE of the same thickness, respectively.

electrification, major factors that determine the surface charge density come from two aspects, i.e., physical morphology and chemical composition.[16,17]

2.3. Origins of Enhancement

First, we employed atomic force microscope (Asylum Research, MFP-3D-SA) to characterize the change of surface roughness. As clearly revealed in Figure 3c,d, drastic contrast of surface undulation can be found as a result of the modification. The unmodified PET surface is very smooth (Figure 3c), which has average roughness (R_a) of 2.2 nm and root mean square roughness (R_q) of 2.8 nm. After the modification, the surface is greatly roughened in nanoscale. The R_a and R_q are found to be 27.4 and 34.4 nm, respectively (Table S1, Supporting Information); and the maximum profile peak height (R_p) reaches 320 nm. The largely magnified roughness results from anisotropic etching by ionic bombardment because of the applied bias voltage.[18]

Second, the surface elemental composition was analyzed by X-ray photoelectron spectroscopy (XPS, Thermo ESCALAB 250Xi). The spectrum of the PET sample before the modification is presented in **Figure 4**a. The entire survey spectrum of the unmodified sample indicates the presence of carbon C1s (284.8 eV, 71.5% atom), oxygen O1s (532.0 eV, 27.9% atom), and a minute amount of fluorine (689.4 eV, 0.6% atom), as listed in Table S2 (Supporting Information). The trace of fluorine is probably because of the introduction of fluorine-containing impurities during synthesis and processing. High resolution spectrum by narrow scan of the C1s peaks is revealed in Figure 4b, which can be deconvoluted into peaks corresponding to C—C (284.8 eV, 66.3% of C1s), C—O (286.3 eV, 18.4% of C1s), and C═O (288.8 eV, 15.3% of C1s, listed in Table S3, Supporting Information). The obtained chemical composition matches well with the molecular formula of bare PET. In contrast, the modification results in high percentage of fluorine (687.5 eV, 37.8% atom, referred to Table S4, Supporting Information), which is 63 times of the unmodified sample as revealed by the survey spectrum in Figure 4c. Moreover, high resolution scan of the C1s peaks in Figure 4d shows clear distinction compared to the unmodified sample. The deconvolution of the C1s peaks exhibits significantly decreased percentage of C—C (from 66.3% to 23.3%), apparently raised percentage of C—O (form 18.4% to 33.9%), relatively stable content of C═O (from 15.3% to 13.3%), and presence of CF (289.2 eV, 9.5% of C1s), CF_2 (291.3 eV, 11.4% of C1s), as well as CF_3 (293.5 eV, 8.6% of C1s, listed in Table S5, Supporting Information). The three peaks centered at 833.1, 860.1, and 878.1 eV correspond to Auger peaks of fluorine, namely KL1, KL2, and KL3, respectively. It becomes apparent that fluorination takes place on the PET surface. The following reaction mechanism is then proposed to describe the fluorination process. Due to plasma discharging, CF_4 gas is decomposed into free radicals such as $\cdot CF_3$ and $:CF_2$ as illustrated by the following reaction equations.

$$CF_4 \rightarrow \dot{C}F_3 + F\cdot \quad (1)$$

$$\dot{C}F_3 \rightarrow :CF_2 + F\cdot \quad (2)$$

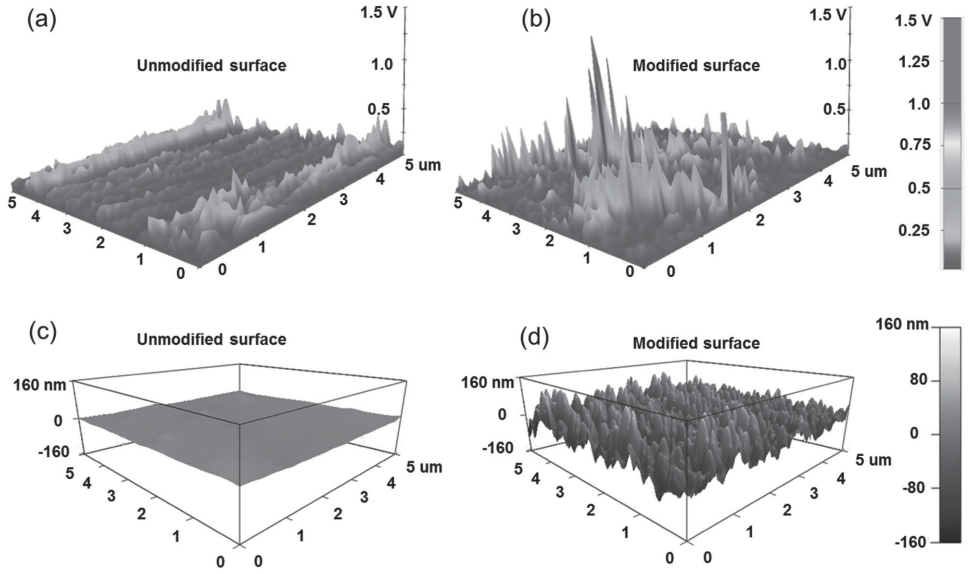

Figure 3. Surface characterization results. Surface electric potential on a) a unmodified and b) a modified PET samples. Surface morphology of c) a unmodified and d) a modified PET samples.

The unstable free radicals ($\cdot CF_3$ and $:CF_2$) tend to recombine into stable CF_4 gas. However, the presence of oxygen in the discharged region can effectively prevent such recombination,[19] producing more $\cdot F$ free radicals, as shown by the reaction equations below.

$$:CF_2 + O_2 \rightarrow \dot{C}OF + F^{\cdot} + \ddot{O} \quad (3)$$

$$\dot{C}OF + \ddot{O} \rightarrow CO_2 + F^{\cdot} \quad (4)$$

The existence of free radicals enables chemical reaction with PET macromolecules. There are two possible reaction routes. The first is "implantation," in which free radicals containing fluorine enable substitution or addition. As shown by the left column in **Figure 5**, they can replace hydrogen or add to pi

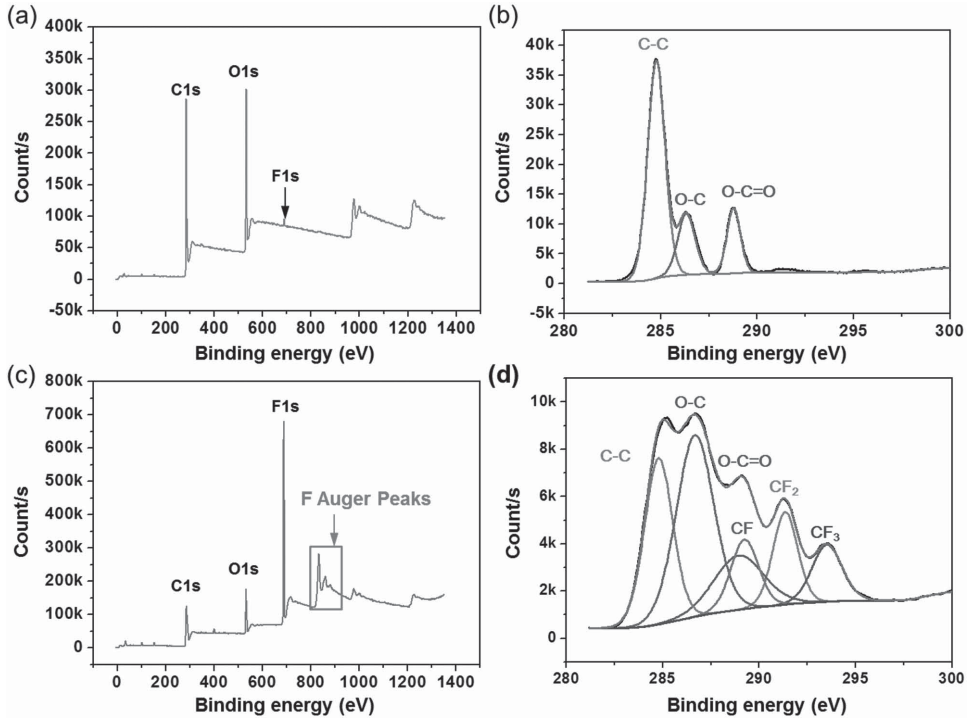

Figure 4. XPS characterization results. a) Survey spectrum on an unmodified PET; b) high-resolution scan and deconvolution of the C1s peak on an unmodified PET; c) survey spectrum on a modified PET; d) high-resolution scan and deconvolution of the C1s peak on a modified PET.

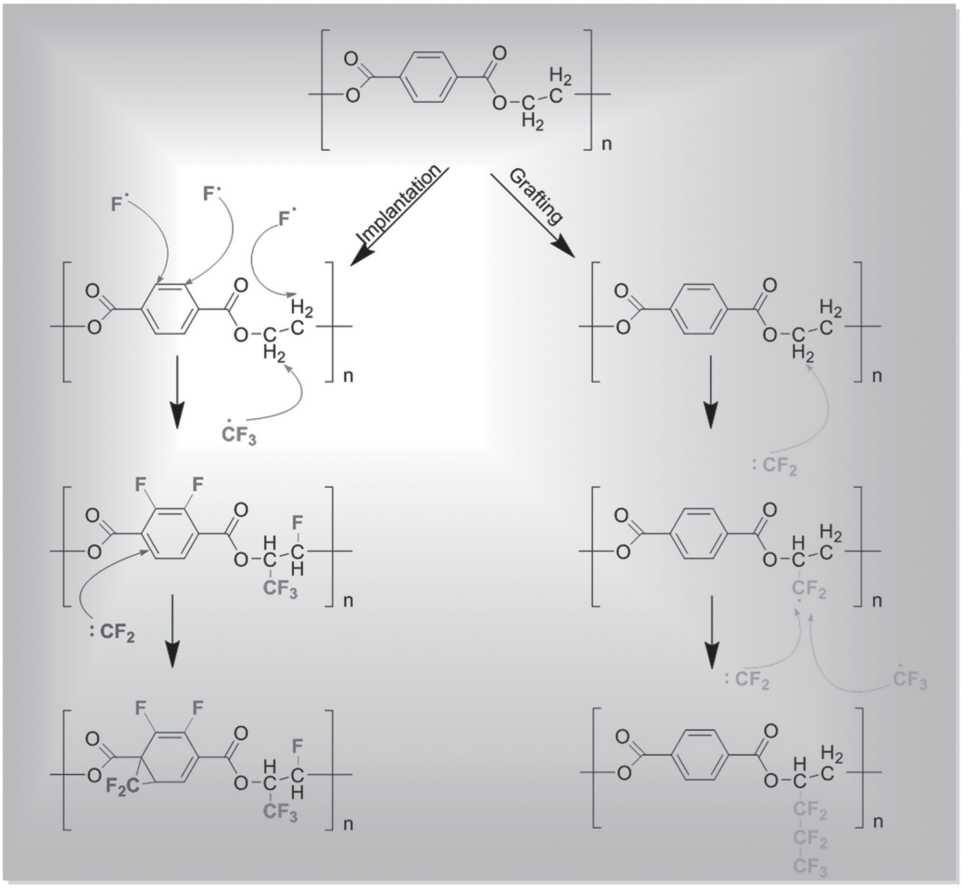

Figure 5. Schematics that illustrate the reactions of fluorination on PET surface.

bonds of the aromatic rings to form reactive saturated intermediates.[20,21] The second is grafting, in which :CF_2 radials form successive chains, as illustrated by the right column in Figure 5.[22]

From the above analysis, the enhanced surface roughness as well as fluorination plays a joint role in promoting the electric output of the TENG. In order to study the mechanical and power output durability of the TENG, we conducted 72000 cycles of continuous test. It was found that the output voltage only reduced by around 2%, as shown in Figure S1 (Supporting Information). Considering the mechanical wear can also cause minor reduction of the electric output, the surface modification is proved to be stable and durable. To distinguish the enhancement effect resulting from each of the mechanism above, we designed two control experiments in which either CF_4 or O_2 was adopted individually in the modification. Detailed etching parameters are presented in Experimental Section. Electrical measurement results are displayed in **Figure 6**a–c. On one hand, the modification by O_2 alone introduces apparently enlarged surface roughness (R_a = 28.7 nm; R_q = 35.9 nm), as shown in Figure 6d and Table S1 (Supporting Information). Although the surface roughness is comparable to that obtained by the CF_4/O_2 plasma, the electric output is much lower than the case where the mixture gas is adopted. This observation is due to the lack of the chemical modification by fluorination. On the other hand, if pure CF_4 was used, the electric output becomes superior to that obtained by the O_2-enabled modification. This is because the CF_4 plasma modifies the PET surface both physically and chemically. However, the enhancement is still lower than that obtained by the mixture gas. This is because the plasma from CF_4 alone creates less surface roughness (R_a = 16.8 nm; R_q = 21.3 nm, as shown in Figure 6e and Table S1, Supporting Information). Besides, less concentration of fluorine-based free radicals are generated without the presence oxygen, which may result in less degree of fluorination. Therefore, the mixture gas is vitally important for the gigantic enhancement effect.

3. Conclusion

In summary, we achieved excellent triboelectric and mechanical properties on the same material for the first time by developing an effective, general, straightforward, and area-scalable approach to modifying PET surface through inductive-coupled plasma etching. The modification enabled gigantic enhancement of triboelectric charge density on the PET surface. By using the modified PET as a contact material, we fabricated TENGs that had significantly promoted electric output. It was

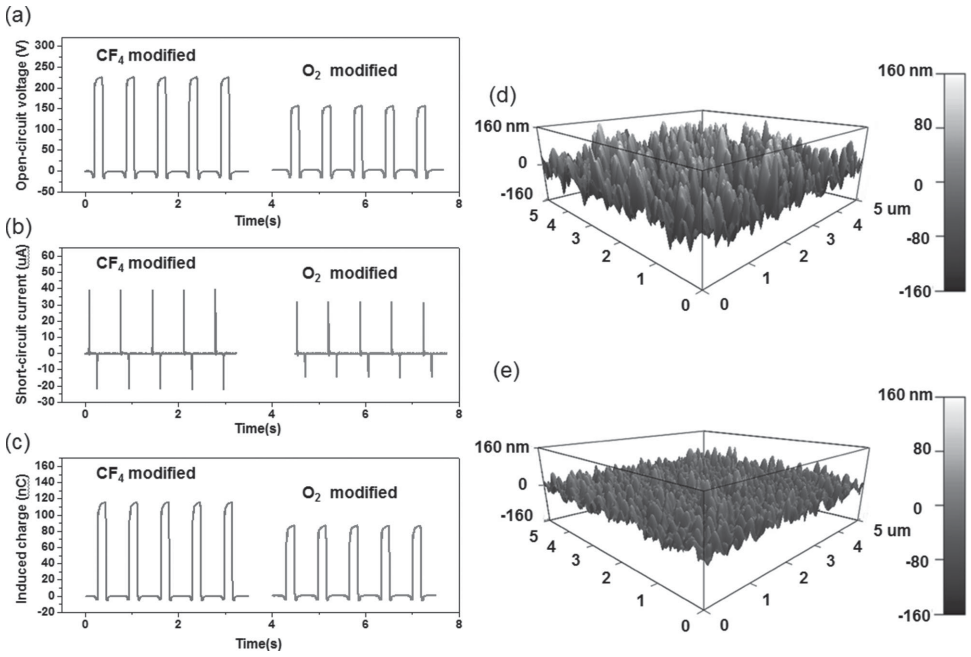

Figure 6. Results of modification by single-component gas in the plasma etching. a) Open-circuit voltage, b) short-circuit current, and c) induced charge quantity of two TENGs that used PET samples solely modified by either O_2 or CF_4, respectively. Surface morphology as a result of the modification by d) O_2 and by e) CF_4.

found that the enhancement of triboelectric charge density was attributed to both chemical modification of fluorination and physical modification of roughened morphology in nanoscale. Therefore, this work proposes a new route to obtaining high-performance TENGs by manipulating and modifying surface properties of materials.

4. Experimental Section

Surface Modification on PET: O_2 and CF_4 gases were introduced into the ICP chamber at flow rates of 10.0 and 30.0 sccm (standard cubic centimeter per minute), respectively. The pressure was 15 mTorr. One power source of 400 W was used to generate high-density plasma while another one of 50 W was used to accelerate plasma ions toward the etched surface. The etching time was 180 s. For modifications solely by either O_2 or CF_4, all parameters kept the same except that the flow rate was set to be 40.0 sccm.

Surface Potential Measurement: First, the contact-mode AFM was used under a normal force of 120 nN to rub the PET surface by Pt-coated tip in a region of 5 μm × 5 μm. Immediately after, the surface potential was measured by KPFM mode. The bias voltage was set to be 3 V and the distance between the top and the surface was 50 nm.

Elemental Composition Measurement: XPS spectra were collected using a monochrome Al Ka (1486.6 eV) at a power 150 W. The binding energy of the adventitious carbon was assumed to be 284.8 eV. The size of the beam spot on the sample was 500 μm.

Supporting Information

Supporting Information is available from the Wiley Online Library or from the author.

Acknowledgements

The research was supported by the "thousands talents" program for pioneer researcher and his innovation team in China. Patents have been filed based on the research presented here.

Received: June 7, 2015
Revised: July 12, 2015
Published online: August 6, 2015

[1] Z. L. Wang, *ACS Nano* **2013**, *7*, 9533.
[2] L. Lin, S. Wang, Y. Xie, Q. Jing, S. Niu, Y. Hu, Z. L. Wang, *Nano Lett.* **2013**, *13*, 2916.
[3] Q. Leng, H. Guo, X. He, G. Liu, Y. Kang, C. G. Hu, Y. Xi, *J. Mater. Chem. A* **2014**, *2*, 19427.
[4] B. Meng, W. Tang, X. Zhang, M. Han, W. Liu, H. X. Zhang, *Nano Energy* **2013**, *2*, 1101.
[5] W. Seung, M. K. Gupta, K. Y. Lee, K.-S. Shin, J.-H. Lee, T. Y. Kim, S. Kim, J. Lin, J. H. Kim, S.-W. Kim, *ACS Nano* **2015**, *9*, 3501.
[6] G. Zhu, J. Chen, Q. Jing, T. Zhang, Z. L. Wang, *Nat. Commun.* **2014**, *5*, 3426.
[7] G. Zhu, Z.-H. Lin, Q. Jing, P. Bai, C. Pan, Y. Yang, Y. Zhou, Z. L. Wang, *Nano Lett.* **2013**, *13*, 847.
[8] X. He, H. Guo, X. Yue, J. Gao, Y. Xi, C. G. Hu, *Nanoscale* **2015**, *7*, 1896.
[9] G. Cheng, L. Zheng, Z.-H. Lin, J. Yang, Z. Du, Z. L. Wang, *Adv. Energy Mater* **2015**, *5*, 1401452.
[10] S. Wang, L. Lin, Z. L. Wang, *Nano Lett.* **2012**, *12*, 6339.
[11] E. C. M. Chen, W. E. Wentworth, *J. Phys. Chem.* **1985**, *89*, 4099.
[12] A. F. Diaza, R. M. Felix-Navarro, *J. Electrostat.* **2004**, *62*, 277.
[13] N. G. Demas, J. Zhang, A. A. Polycarpou, J. Economy, *Tribol. Lett.* **2008**, *29*, 253.

[14] Z. Zhang, P. Klein, K. Friedrich, *Compos. Sci. Technol.* **2002**, *62*, 100.
[15] P. Bai, G. Zhu, Y. Zhou, S. Wang, J. Ma, G. Zhang, Z. L. Wang, *Nano Res.* **2014**, *7*, 990.
[16] B. Jin, B.-M. Wilén, P. Lant, *Chem. Eng. J.* **2004**, *98*, 115.
[17] S.-H. Shin, Y. H. Kwon, Y.-H. Kim, J.-Y. Jung, M. H. Lee, J. Nah, *ACS Nano* **2015**, *9*, 4621.
[18] V. C. Rucker, K. L. Havenstrite, B. A. Simmons, S. M. Sickafoose, A. E. Herr, R. Shediac, *Langmuir* **2005**, *21*, 7621.
[19] S. Raoux, T. Tanaka, M. Bhan, H. Ponnekanti, M. Seamons, T. Deacon, L.-Q. Xia, F. Pham, D. Silvetti, D. Cheung, K. Fairbairn, A. Jonhson, R. Pearce, J. Langan, *J. Vac. Sci. Technol. B* **1999**, *17*, 477.
[20] P. Scott, L. Matienzo, S. V. Babu, *J. Vac. Sci. Technol. A* **1990**, *8*, 2382.
[21] L. Zhang, W. Chin, W. Huang, J. Q. Wang, *Surf. Interface Anal.* **1999**, *28*, 16.
[22] W. Xiang, X. Chen, J. Q. Wang, *J. Polym. Sci., Polym. Chem.* **1995**, *33*, 807.